C. Barth, O. H. Pakarinen, A. S. Foster, and C. R. Henry, Imaging nanoclusters in the *constant height mode* of the dynamic SFM, Nanotechnology 17, S128 (2006).

INSTITUTE OF PHYSICS PUBLISHING NANOTECHNOLOGY
Nanotechnology **17** (2006) S128–S136 doi:10.1088/0957-4484/17/7/S05

Imaging nanoclusters in the *constant height mode* of the dynamic SFM

Clemens Barth[1,3], **Olli H Pakarinen**[2], **Adam S Foster**[2] **and Claude R Henry**[1]

[1] CRMCN-CNRS, Campus de Luminy, Case 913, 13288 Marseille Cedex 09, France[4]
[2] Helsinki University of Technology, Laboratory of Physics, PO Box 1100, FIN-02015 HUT, Finland

E-mail: barth@crmcn.univ-mrs.fr

Received 21 August 2005, in final form 20 January 2006
Published 10 March 2006
Online at stacks.iop.org/Nano/17/S128

Abstract
For the first time, high quality images of metal nanoclusters which were recorded in the *constant height mode* of a dynamic scanning force microscope (dynamic SFM) are shown. Surfaces of highly ordered pyrolytic graphite (HOPG) were used as a test substrate since metal nanoclusters with well defined and symmetric shapes can be created by epitaxial growth. We performed imaging of gold clusters with sizes between 5 and 15 nm in both scanning modes, constant Δf mode and constant height mode, and compared the image contrast. We notice that clusters in constant height images appear much sharper, and exhibit more reasonable lateral shapes and sizes in comparison to images recorded in the constant Δf mode. With the help of numerical simulations we show that only a microscopically small part of the tip apex (nanotip) is probably the main contributor for the image contrast formation. In principle, the constant height mode can be used for imaging surfaces of any material, e.g. ionic crystals, as shown for the system Au/NaCl(001).

(Some figures in this article are in colour only in the electronic version)

1. Introduction

The study of metal nanoclusters deposited on oxide surfaces forms a large domain in catalysis, since these model systems provide great insight into the nature of fundamental catalytic reactions [1, 2]. A characterization of the clusters concerning their structure and morphology is of utmost importance, and has previously been done mainly by high resolution TEM [3] and STM [3, 4]. For an *in situ* characterization and for substrates of insulating materials such as MgO or Al_2O_3, only the scanning force microscope can be used. Especially in its dynamic mode, the SFM offers in principle the ability to image surfaces with high resolution—in the best case with atomic resolution [5–7].

However, for a characterization of the cluster size and shape, the scanning force microscope was mainly used in the contact mode [8, 9]. In this mode, the tip apex strongly influences the shape and size of small clusters in the images due to tip convolution [10–13] which can be partially reduced by numerical reconstruction [14, 15]. Only a few works can be found in the literature which deal with dynamic SFM imaging of nanoclusters so far [16–18]. Recently, we started to study the contrast formation in dynamic SFM of nanoclusters which were imaged in the topography imaging mode. We found out that the tip apex is also the main limiting factor [19, 20]—similar to the characteristics appearing in the contact mode [10]: as soon as the cluster size is smaller than the tip apex, the tip is mostly imaged [19].

In this paper we propose to use another scanning mode of the dynamic SFM for imaging nanoclusters—the *constant height mode*. This mode is similar to the one frequently used in scanning tunnelling microscopy (STM), especially for *real time* STM [21, 22], and was already introduced in dynamic SFM for atomic resolution imaging of insulating surfaces [23]. It is a complementary scanning mode to the

[3] Author to whom any correspondence should be addressed.
[4] The CRMCN is associated with the University of Aix-Marseille II and III.

topography imaging mode, which images the lateral shape and size of nanoclusters.

We recorded images in the constant height mode of the dynamic SFM of gold nanoclusters grown on HOPG with the tunnelling current and the detuning as the feedback signal. This surface served as a test system, offering small clusters with well defined, symmetric shapes. We could observe a significant improvement of the image quality in constant height images. The clusters exhibit lateral shapes and sizes which are more physically representative than the ones which can be seen in topography images of the same clusters. We show that the high quality is likely due to a strong tip–surface interaction between an atomistic small part of the tip, called the *nanotip*, and the cluster. Due to the nanotip, the tip convolution effect is reduced to a large extent.

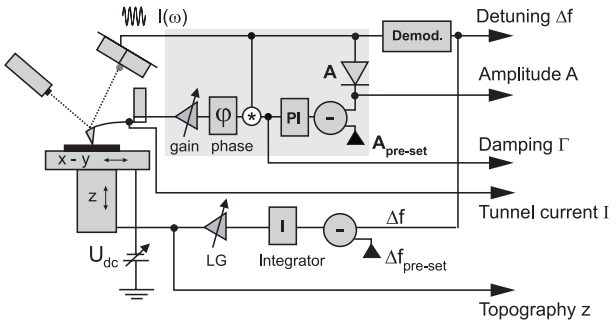

Figure 1. Principle of a dynamic SFM. Note that the drawing above is only a simplified diagram of the function principles. Detailed and precise circuits of the electronics can be found in [31, 32].

2. Experiment

2.1. Samples and instruments

HOPG samples were bought from Union Carbon Corporation (UCAR, USA) and cleaved in air prior to their transfer into UHV. The samples were further annealed in UHV at 400 °C overnight in order to remove possible contaminants from the surface. Crystals of NaCl had a purity of ∼99.5% and were produced in our laboratory by the Czochralski growth method in a similar way as described in [24, 25]. The surfaces of the crystals were prepared by UHV cleavage at room temperature parallel to the (001) cleavage plane with high precision [26]. After cleavage the crystals were annealed in a UHV oven at 100 °C for 30 min in order to reduce charging after cleavage [26, 27].

Gold clusters were epitaxially grown by condensing a calibrated beam of neutral gold atoms from a Knudsen cell on HOPG and NaCl(001) surfaces at a temperature larger than 450 and at 200 °C, respectively. We used a constant flux of neutral gold atoms of 1×10^{13} atoms cm^{-2} s^{-1} (no nucleation of clusters in the gold beam).

Scanning force experiments were performed at room temperature in UHV ($\sim 10^{-10}$ mbar base pressure) with a dynamic SFM (Omicron STM/AFM) equipped with a digital demodulator (Nanosurf). Dynamic SFM measures the change in frequency (detuning Δf) of an oscillating cantilever due to the interaction of a tip at the end of the cantilever with the surface [5–7]. Before taking measurements, the fast scanning direction was changed during scanning in the constant Δf mode by an adjustment of the scanning angle until the fast scanning direction was parallel to the surface with an error of a few degrees. We used p-doped silicon cantilevers (1.5 Ω cm, Nanosensors) which we did not sputter before experiments, and hence were oxidized by exposure to the ambient. The tips were regularly in contact with the surface before taking images, so that the tip apex was most probably covered by a thin silicon oxide layer and with material of the surfaces.

2.2. Imaging modes

The set-up of our SFM is based on the beam-deflection principle [28] and equals the design of Howald *et al* [29]. The dynamic mode of the SFM is realized as described in [30] and further characterized in [31, 32]. With the help of figure 1 we give a brief overview of the main signals of the control loops to which we refer throughout the paper. Afterward, a description of the constant Δf and constant height mode is given.

The force microscope has basically two independent control loops, the amplitude control loop (top grey box) and the distance control loop (remaining components). The amplitude control loop is based on the self-excitation principle and keeps the amplitude A constant on its pre-set value $A_{\mathrm{pre-set}}$, whereas the energy per cycle which must be put into the system is called damping (Γ). More details regarding the damping can be found in [32] and in the references therein.

Depending on the feedback mode that is chosen, the distance control loop measures either the detuning Δf of the free cantilever oscillation (detuning feedback mode) or the tunnel current I (current feedback mode) which is taken from the tip and which can be used only for conducting materials. The tunnel current is thereby averaged over several cycles of the cantilever oscillation [33]. The characteristics of the distance control loop is similar for both feedback modes and we describe them with the help of the detuning feedback mode in the following. For the current feedback mode, the parameters Δf and $\Delta f_{\mathrm{pre-set}}$ must only be changed by I and $I_{\mathrm{pre-set}}$ (pre-set value of the current), respectively.

The actual detuning is compared with a pre-set value $\Delta f_{\mathrm{pre-set}}$, amplified by the integrator (I) and the loop gain (LG) and coupled to the z-piezo of the scanner. The voltage at the z-piezo is translated into a distance and yields the topography signal (Z). The extent to which the distance control loop keeps the detuning Δf constant does strongly depend on the loop gain and on the scanning speed v_{Scan}. If the scanning speed is low ($v_{\mathrm{Scan}} < 1$–2 Hz) and the loop gain high, changes in the detuning Δf which appear during scanning are on a timescale which is similar to the time response τ of the integrator and loop gain, and the detuning is kept constant at $\Delta f_{\mathrm{pre-set}}$ by an adjustment of the tip–surface distance Z. The tip follows the contours of the surface topography (pathway (1) in figure 2). All information on the tip–surface interaction is included in the topography image, whereas the detuning image shows a uniform contrast with only residual, small changes of the detuning in the range of a few per cent and less. This scanning mode is frequently called the topography imaging mode or *constant Δf mode* and is explained more in detail for the imaging of clusters by Fain and co-workers [34]. In the following, we call corresponding images *constant Δf images*.

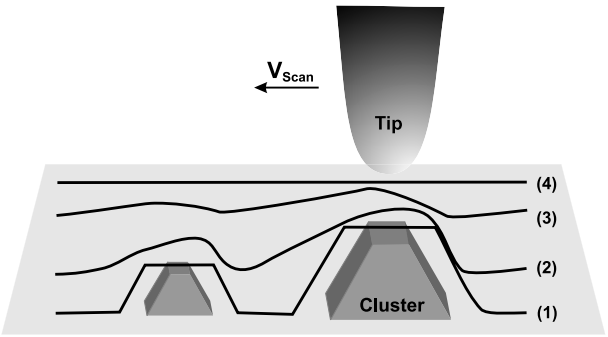

Figure 2. A drawing explaining the differences between the constant Δf mode (1) and the constant height mode (4). Pathways (2) and (3) correspond to intermediate scanning conditions between both modes.

If the tunnelling current is used as the feedback signal, the scanning mode and corresponding images are called *constant current mode* and *constant current images*, respectively.

As soon as the loop gain decreases and/or the scanning speed increases, the distance control loop is no longer capable of regulating on constant detuning $\Delta f = \Delta f_{\mathrm{pre-set}}$. The finite time response τ is larger than the time in which changes in Δf appear. The result is that the tip only partially follows the topography (pathways (2) and (3) in figure 2). The longer the time response, the more the topography becomes blurred and the more a contrast in the Δf image develops. Further, due to the long integral response of the distance control loop, a *memory* of the tip pathway is present so that the cluster profiles in Z along the fast scanning direction become asymmetric, which we will explain in detail in section 3.1.

For very small loop gains and high scanning speeds, the tip follows only the inclination of the surface with respect to the fast scanning direction (pathway (4) in figure 2) and, in the extreme case, only in the surface plane. The detuning image then includes all information on the tip–surface interaction, whereas the topography image includes only the surface plane, which is mostly inclined to the fast scanning direction. The latter scanning mode is frequently called *constant height mode* for both feedback modes. Corresponding images are called *constant height images* in the following.

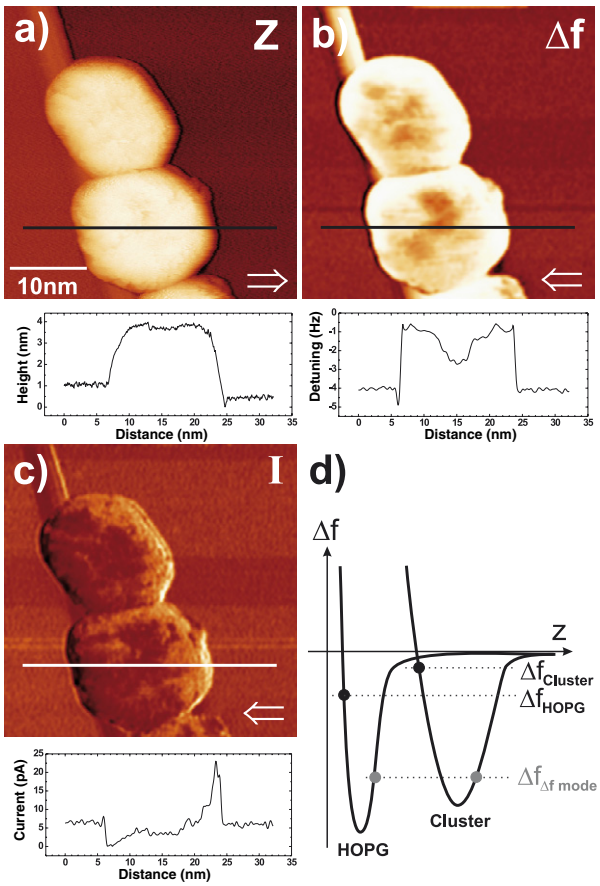

Figure 3. Gold clusters on HOPG imaged in the constant I mode with the tunnelling current as the feedback signal. The images show the topography Z (a), detuning Δf (b) and tunnelling current I (c). All images were slightly FFT filtered except the topography image. The arrows indicate the fast scanning direction. (d) Drawing of the detuning versus distance curves above HOPG and the clusters. $\Delta f_{\Delta f\,\mathrm{mode}}$ is the pre-set value of the detuning for the measurement shown in figure 5. Gold with a nominal thickness of 3 ML was deposited at 500 °C with additional annealing for 10 min at 500 °C. (37×37 nm^2, $I_{\mathrm{pre-set}} = 0.01$ nA (mean value), $U_{\mathrm{DC}} = 0.5$ V, LG = 6.7, $v_{\mathrm{Scan}} = 100$ nm s^{-1} (2.7 Hz), $f_0 = 267.9$ kHz, $k = 32$ N m^{-1}, $A_{\mathrm{p-p}} = 6.4$ nm.)

3. Loop characteristics

In this section we discuss and compare the main features in images of the signals z, Δf and I which were recorded in the constant current and detuning mode with the same types of images recorded in the constant height mode. Since HOPG is a conductor, we first used the tunnelling current as the feedback signal of the distance control loop. Then we show that constant height mode imaging can also be performed if the detuning Δf is used as a feedback signal.

3.1. Current feedback mode

In the first set of experiments we used the tunnelling current I as the feedback signal for the distance control loop for imaging gold clusters on the HOPG surface. In figure 3 three images of the signals Z (a), Δf (b) and I (c) are shown, which were recorded simultaneously during one measurement in the constant I mode. During scanning, the scanning speed and loop gain[5] were adjusted so that the tunnelling current was nearly constant at each position in the image. The image of the tunnelling current shows only slight changes from the pre-set value $I_{\mathrm{pre-set}}$.

The topography image in figure 3(a) shows two clusters which are attached at a cleavage step of HOPG. They appear with an apparent mean size of ∼15 nm and a height of ∼2.5 nm and exhibit relatively flat top facets with straight edges. The detuning image (b) also shows a strong contrast of the clusters with similar lateral shapes. The detuning above the clusters is smaller ($\Delta f_{\mathrm{Cluster}} = -1$ Hz) than above the HOPG surface ($\Delta f_{\mathrm{HOPG}} = -4$ Hz), so that it seems that the tip–cluster distance was larger than the one above the HOPG surface. However, due to the very small tip–surface distances, which

[5] The scale for the loop gain of our dynamic SFM is logarithmic. The values mentioned in this paper are the same as the ones which are used for the remote control of the SFM.

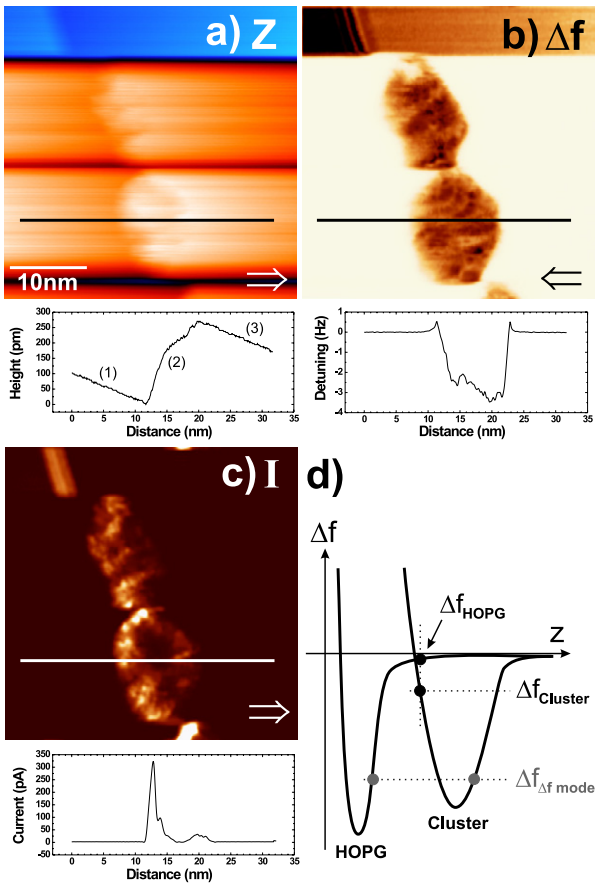

Figure 4. The same gold clusters as in figure 3 imaged in the constant height mode. The tunnelling current was again the feedback signal. The images show the topography Z (a), detuning Δf (b) and tunnelling current I (c). The arrows indicate the fast scanning direction. (d) Drawing of the detuning versus distance curve above HOPG and the clusters. $\Delta f_{\Delta f\ \mathrm{mode}}$ is the pre-set value of the detuning for the measurement shown in figure 5. (37×37 nm^2, $I_{\mathrm{pre-set}} = 0.01$ nA (mean value), $U_{\mathrm{DC}} = 0.5$ V, LG $= 0.05$, $v_{\mathrm{Scan}} = 200$ nm s^{-1} (5.4 Hz), $f_0 = 267.9$ kHz, $k = 32$ N m^{-1}, $A_{\mathrm{p-p}} = 6.4$ nm).

are kept in a range of some ångströms during normal regulation on the tunnelling current, the tip was already in the repulsive part of the detuning as shown by the detuning versus distance curves in (d). The contrast in the display of the data is then inverted, so that smaller detuning values mean effectively smaller tip–surface distances. As will be shown in section 3.2, a detuning of $\Delta f_{\Delta f\mathrm{mode}} = -23$ Hz was needed to image clusters in the detuning feedback mode with the same tip, where the tip was in the attractive part of Δf.

After the measurement above we performed measurements in the constant height mode above the same clusters (figure 4). We first increased the tip–surface distance by reducing the pre-set value of the tunnelling current during scanning. The tip was then at a safe distance to the surface during the following increase and decrease of scanning speed and loop gain, respectively. Afterward, the pre-set value for the tunnelling current was carefully increased until a contrast of the clusters could be seen in the images.

For the measurement in figure 4, a twice as high scanning speed was used and the loop gain was reduced from 6.7 to 0.05. The time response of the distance control loop was therefore much smaller by orders of magnitude than before. Only changes of several hundreds of picometres can be seen in the topography image (a) within single scanning lines, which is about one-tenth as high as the apparent cluster height of 2.5 nm in the constant current image in figure 3(a).

The residual contrast in the topography image figure 4(a) shows that the distance control loop was obviously able to regulate on changes of the tunnelling current to a small extent during scanning. The features in the image are typical for a regulation with a very long time response of the distance control loop. First, the image shows a fuzzy dark/bright contrast at the edges of the clusters perpendicular to the scanning direction. This is mainly due to three sections of linear tip pathways (1–3), as can be seen in the corresponding profile below the topography image (a). Since the feedback signal I is nearly constant, but different from its pre-set value in each section, the integration in each section yields a straight tip pathway with a slope which changes after each drastic change of the current. Only straight tip pathways are visible, since the distance control has no time to regulate the current I on its pre-set value due to the long time response τ in comparison to the fast changes in I. Due to a memory effect of the distance control loop, the latter scanning characteristic strongly depends on the fast scanning direction in that an inverted contrast at the edges can be observed in the topography image of the reversed fast scanning direction (not shown).

The second type of image feature, which is typical for imaging with large time responses of the distance control loop, is stripes and regions parallel to the fast scanning direction (dark stripes and the blue region in image (a)) in which the mean height is much lower than the one of regions above the clusters. Profiles taken in the blue region (not shown) exhibit that the tip was approached to the surface to a distance of ∼2.5 nm. The reason is that as soon as the tip completely passes a cluster, the tip scans only above the HOPG surface. Although the time response of the distance control loop is very long for one scanning line, it is comparable, however, with the time needed to pass several scanning lines during scanning. As a consequence the tip approaches the HOPG surface by a distance which equals the height of the clusters after a couple of scanning lines. In the latter case, features of the HOPG surface are imaged—such as the cleavage step in the blue region, which can also be observed in the detuning (b) and current (c) images.

In contrast to the topography image in figure 4(a), the detuning image in (b) presents much more detail of the lateral cluster shape and size. The size and shape are different in comparison to those in the images which were taken in the constant I mode (figure 3) on which we will concentrate in section 4.1. The detuning image exhibits no detuning above the HOPG surface on the left and right sides of the clusters ($\Delta f_{\mathrm{HOPG}} \approx 0$). In these surface regions the tip was too far away to detect a tip–surface interaction, and this is also confirmed by the current image (c), where the current is zero in the same surface regions. Above the clusters, the detuning is indeed negative, but very small ($\Delta f_{\mathrm{Cluster}} = -3$ Hz). Tunnelling currents of 50–300 pA can be observed in the image of the current (c). Also here, the detuning values above the clusters

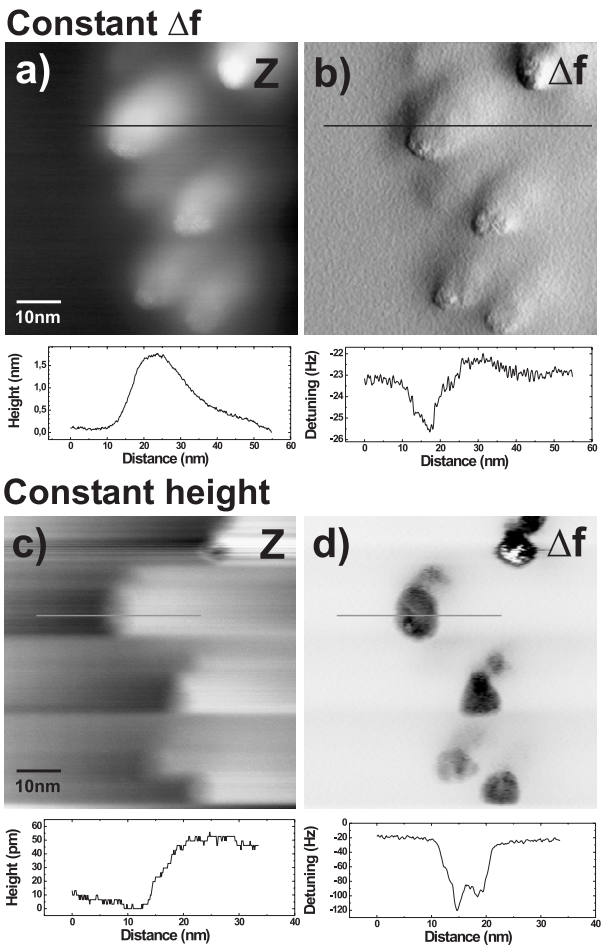

Figure 5. Gold clusters on the same HOPG surface as shown in figures 3 and 4, but taken from a different surface region. The clusters were imaged in the constant Δf ((a) and (b)) and constant height mode ((c) and (d)), with the detuning Δf used as the feedback signal. The fast scanning direction was from left to right for all images. (60×60 nm^2, $\Delta f = -23$ Hz, $U_{\mathrm{DC}} = 0.4$ V, $f_0 = 267.9$ kHz, $k = 32$ N m^{-1}, $A_{\mathrm{p-p}} = 6.4$ nm; (a) and (b) LG = 6.2, $v_{\mathrm{Scan}} = 200$ nm s^{-1} (3.3 Hz); (c) and (d) LG = 0.01, $v_{\mathrm{Scan}} = 510$ nm s^{-1} (8.5 Hz).)

were due to a very short tip–cluster distance where the tip was already in the repulsive part of the detuning $\Delta f(z)$ as shown by the detuning versus distance curves in (d).

3.2. Detuning feedback mode

We repeated similar measurements on the HOPG surface, but with the detuning Δf as the feedback signal for the distance control loop (figure 5). The same tip and surface was used as for the experiments presented in section 3.1.

First, we performed a measurement in the constant Δf mode ((a), (b)). During scanning, the tip was approached as close as possible to the surface. The topography image (a) was taken at a detuning of $\Delta f_{\Delta f\,\mathrm{mode}} = -23$ Hz with a high loop gain, so that only a residual contrast in the image of the detuning (b) is visible. Much smaller detunings did not result in significantly better contrast of topography images than those in (a). The detunings of a few hertz in figures 3(b) and 4(b) were therefore due to a short tip–surface distance, where the tip was already in the repulsive region of $\Delta f(z)$. Note that the reason that figure 3(a) is much better than figure 5(a) is that the averaged tunnelling current decays with distance much faster than the detuning.

The topography image in figure 5(a) shows a group of clusters with apparent cluster sizes of ∼10 nm and a mean cluster height of ∼1.5 nm. The clusters appear as round and rather fuzzy objects, which is due to the influence of the finite tip size in the contrast formation [19]. In particular, the *tail* at the top of each cluster, which makes an angle of 45° with the fast scanning direction, is a sign of a tip convolution effect. However, the tip was obviously sharp at the nanometre scale and close enough to the clusters since flat top facets with partially triangular shapes of some clusters can be roughly estimated, e.g. in (b).

After this measurement, we performed one in the constant height mode which is shown in figures 5(c) and (d). Similarly as described in section 3.1, we first retracted the tip during scanning in the constant Δf mode by using much less negative pre-set detuning values. The scanning frequency was then doubled and the loop gain decreased from 6.2 to 0.01, so that the time response of the distance control loop was again very slow. The tip was then approached to the surface by choosing more negative pre-set values for the detuning as long as a contrast in the images could be seen.

The topography image (c) shows only subtle contrast changes of about 50 pm. The specific tip movement of straight pathways is similar to that in figure 4(a) as discussed in section 3.1. Note that a mean subtraction routine[6] was used for this topography image for increasing the residual contrast of the image.

In contrast to the topography image, the detuning image (d) includes all information on the tip–surface interaction. It can be clearly seen that the clusters appear with highest quality. The strong contrast is due to a detuning of more than −100 Hz at the clusters, which is much more negative than the detuning above the HOPG surface, which measures −20 Hz. Note that, here, the tip was always in the attractive part of the tip–surface interaction $\Delta f(z)$, so that the detuning above clusters is more negative (dark) than above the HOPG surface (bright), which is the opposite case in comparison to the situation described in section 3.1.

3.3. Advantages and limits of the constant height mode

Although the surface height information gets lost in the constant height mode, it is not a serious disadvantage. The approximate height information can be obtained in the constant Δf or constant current mode, which completes the whole set of information. In fact, the constant height mode has rather a big advantage, in that images with a high quality can be gained. The images exhibit a higher contrast with well defined lateral shapes in the constant height mode than in any other mode. Further, in all cases the clusters have a reduced size in constant height images compared to constant Δf images, which points out that the tip convolution effect is minimized. We will focus on this issue in section 4.

[6] The mean routine calculates the mean Z-value of each scanning line and subtracts these from the respective scanning line of the original data [31].

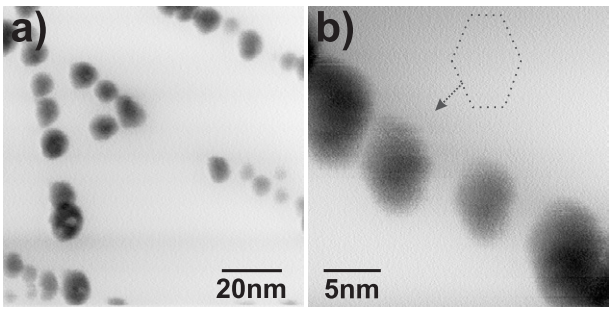

Figure 6. Gold clusters deposited on the NaCl(001) surface (0.6 ML gold at 170 °C). The clusters were imaged in the constant height mode with the detuning as the feedback signal. They are attached at cleavage steps of the NaCl(001) surface. The fast scanning direction was from left to right for both images. ((a) 100×100 nm^2, $\Delta f = -51.6$ Hz, $v_{\mathrm{Scan}} = 1502$ nm s^{-1} (15 Hz); (b) 26×26 nm^2, $\Delta f = -51$ Hz, $v_{\mathrm{Scan}} = 302$ nm s^{-1} (11.5 Hz); all, $U_{\mathrm{DC}} = 3.3$ V, LG = 0.1, $f_0 = 274.4$ kHz, $k = 44$ N m^{-1}, $A_{\mathrm{p-p}} = 13.6$ nm.)

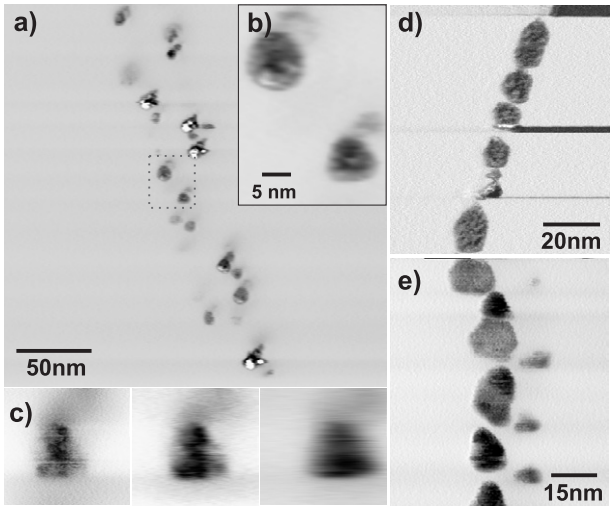

Figure 7. Constant height images (Δf feedback mode) of clusters in the same surface region as in figure 3 except (e) which was taken on another HOPG surface (5 ML Au at 360 °C + additional annealing for 10 min at 360 °C). (a), (b) Large scale image (250×50 nm^2). Image (b) is a cut-out that was taken at the position of the dotted square in image (a). (c) Cluster with triangular shape imaged with different scanning speeds (13, 65, 195 Hz). The fast scanning direction was from left to right for all images. ((a)–(c) $U_{\mathrm{DC}} = 0.4$ V, LG = 0.2, $f_0 = 267.9$ kHz, $k = 32$ N m^{-1}, $A_{\mathrm{p-p}} = 6.4$ nm; (a), (b) $\Delta f = -18.2$ Hz, $v_{\mathrm{Scan}} = 6.3$ Hz; (c) 15×15 nm^2, $\Delta f = -21.8$ Hz; (d) $\Delta f = -51.6$ Hz, $U_{\mathrm{DC}} = 3.3$ V, LG = 0.1, $v_{\mathrm{Scan}} = 15$ Hz, $f_0 = 274.4$ kHz, $k = 44$ N m^{-1}, $A_{\mathrm{p-p}} = 13.6$ nm; (e) $\Delta f = -20.4$ Hz, $U_{\mathrm{DC}} = -0.02$ V, LG = 0.1, $v_{\mathrm{Scan}} = 9.8$ Hz, $f_0 = 70.9$ kHz, $k = 2.8$ N m^{-1}, $A_{\mathrm{p-p}} = 35$ nm.)

The constant height mode can be used in principle for surfaces of any material and cluster size. We also tested the application of the constant height mode for surfaces of insulators like on the (001) surface of NaCl on which we deposited 0.6 ML of gold at 170 °C. The image in figure 6(a) also shows the same high quality contrast of clusters as in the case of Au/HOPG. In images with a higher magnification (b) the lateral shape of some clusters can be clearly seen—the labelled cluster forms an elongated hexagon, probably due to a three-dimensional cluster shape of a truncated octahedron on a threefold symmetry axis, which is known to occur at the early stage of epitaxy of gold on NaCl(001) [35].

Independent of the feedback signal Δf or I, imaging with a much larger scanning frame can be performed without crashing the tip into the surface as shown by the large scale image (250×250 nm^2) in figure 7(a), which was taken on HOPG. Amazingly, high resolution can be achieved even with such large scanning frames, as can be seen by the cut-out in (b) which was taken at the position of the dotted square in image (a). The cluster with the triangular shape is the same cluster as in the images in figure 5 and shows similar details to image figure 5(d).

The much better contrast in constant height images in comparison to constant Δf images is only one advantage. Another advantage of the constant height mode is the high scanning speed, which minimizes the influence of the instrumental drift in the images. The scanning speed is mainly limited by the frequency f_0 of the cantilever oscillation. The triangular cluster in image figures 5(d) and 7(b) was imaged with three high scanning speeds: 13, 65, 195 Hz. The corresponding images in figure 7(c) show that the cluster becomes more blurred with increasing speed, especially at the highest speed of 195 Hz. At the latter speed the tip stays only for $1/(195 \times 512) = 10$ μs above one pixel for an image with 512×512 pixels. This time is comparable to one period of the cantilever oscillation ($1/f_0 = 1/268$ kHz $= 3.73$ μs) so that the tip performs only 2.7 periods for one pixel. If $n = 512$ is the number of pixels for a scanning line and if ten periods are taken as the smallest periods per pixel for a reasonable contrast (equals image in (c) taken at -65 Hz), then we get $v_{\mathrm{Scan}} = f_0/(10 \times n) \approx 60$ Hz and 15 Hz as the highest scanning speeds for 300 and 70 kHz tips, respectively, which are still amazingly large values.

4. Image analysis

The main question that arises is whether the real lateral cluster shapes and sizes are imaged in the constant height mode. In the following, we first compare two images recorded in the constant I and height mode of the same clusters, and comment on the tip convolution effect. Then we compare the lateral cluster shapes with those previously observed in TEM images exhibiting the correct lateral shapes and sizes. Finally, we comment on how the contrast formation of clusters is realized and to what extent the tip convolution effect is reduced in the constant height mode.

4.1. Comparison

For a comparison of lateral cluster sizes and shapes, we examine the topography image in figure 3(a) recorded in the constant current mode and the detuning image in figure 4(b) recorded in the constant height mode.

The main observation is that the clusters appear wider in the topography image in figure 3(a) than in the detuning image in figure 4(b), especially in the horizontal direction. Vertically, the cluster length is equal in both images (15 nm); however, horizontally, both clusters have a width which is about 5 nm larger in the topography image than in the detuning image. Note that the broadening of the clusters in figure 3(a)

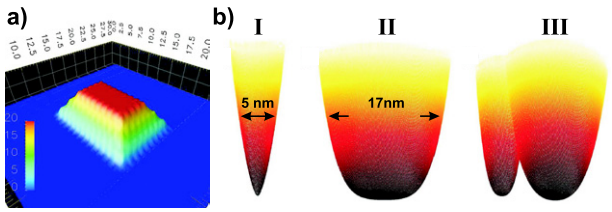

Figure 8. (a) Truncated pyramidal cluster ($8 \times 12 \times 2$ nm^3) used in simulating tip convolution (xy- and z-coordinates in nanometres and ångströms, respectively). (b) The different tip models considered: (I) sharp tip, (II) blunt tip, (III) asymmetric tip. The height of the tips measures 22 nm. The tip shapes are defined as being proportional to different polynomial shapes, with the following forms: sharp tip $y = x^{1.6}$; blunt tip $y = x^4$; asymmetric tip $y = x^3$. The asymmetric tip is formed by combining two polynomial tips where the smaller one is shorter by 1 nm.

was coincidentally parallel to the scanning direction and not due to a too slow time response of the distance control loop; the topography images in the forward scanning direction (figure 3(a)) exhibit the same image details as the topography image in the backward scanning direction (not shown).

The cluster lateral shapes and sizes in the detuning image are supposed to be the correct ones; the clusters in the topography were then imaged with an asymmetric tip, where the apex had a more elongated lateral shape in the horizontal direction.

In general, the measurements in figures 3 and 4 and many other images (not shown) show that the clusters always appear smaller in constant height images than in corresponding topography images. The cluster sizes are reduced by up to 50%, which is a typical convolution factor as shown by a comparison of contact SFM and TEM images [13]. Further, most of the constant height images show lateral cluster shapes which are comparable to previous TEM measurements [36–38], on which we will concentrate in the following.

Different and precisely formed lateral shapes of the clusters can be identified on HOPG: aside from some complex cluster shapes, polygonal shapes such as triangles, pentagons and hexagons can be mainly observed in the images. Triangular clusters only appear rarely, e.g. in figure 5(d), which is due to the large average cluster size of more than 5 nm. As has been shown before for supports with a threefold symmetry axis, the clusters grow in the (111) epitaxy and have a three-dimensional tetrahedral shape [8, 36], which they keep up to sizes of a few nanometres [2]. Clusters with larger sizes than 5 nm exhibit different equilibrium shapes, namely truncated tetrahedrons [2], as shown by TEM and STM [36–38]. Clusters with these three-dimensional shapes are mostly imaged as hexagons with the force microscope, which is in agreement with the lateral shapes we found in our images as shown in figures 7(d) and (e). However, due to an unfinished growth to the hexagonal cluster shape at equilibrium and due to a coalescence of clusters at high temperatures, the lateral cluster shape can deviate from the ideal hexagonal shape so that pentagonal and more complex lateral cluster shapes appear (see images in figures 7(d) and (e)) [2].

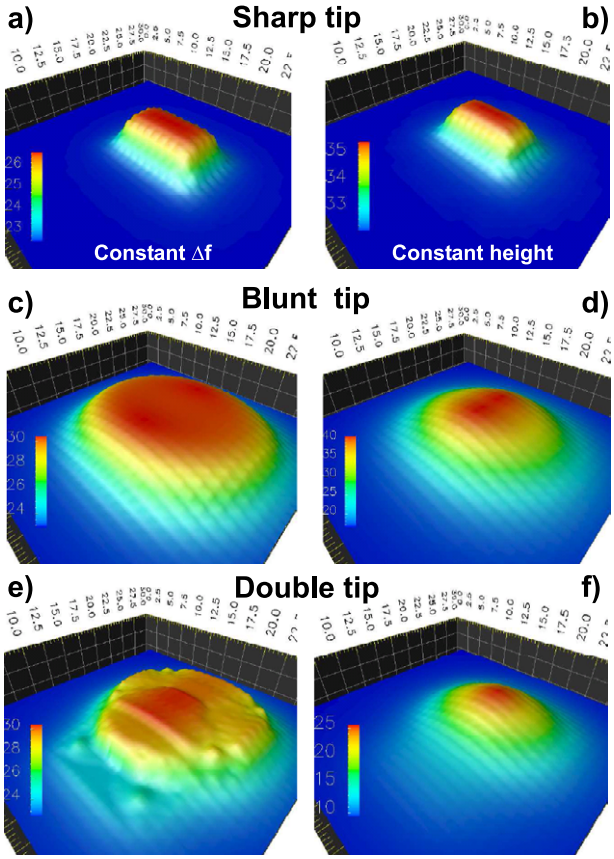

Figure 9. Images of the cluster in figure 8(a) calculated with the three types of tips (sharp, blunt and double tips) shown in figure 8(b) for constant Δf and height modes. Images on the left ((a), (c), (e)) are topography images, the ones on the right detuning images. The detuning images were simulated at -45 Hz (a), -30 Hz (c) and -45 Hz (e). The constant height images were simulated at a distance of 3 nm from the substrate surface.

4.2. Contrast formation

Following the experimental comparison, we now try to explain the image contrast formation and the tip convolution effect from a theoretical point of view. Since we are not interested in atomic contrast and we know that van der Waals forces dominate the attractive tip–surface interaction at nearly all tip–surface distances [20], for this study we consider only the van der Waals force between the tip and cluster. We performed numerical simulations in which we consider three tip models imaging a cluster on the surface. The cluster shown in figure 8(a) has a truncated pyramidal shape and a size of $8 \times 12 \times 2$ nm^3—a similar dimension to the clusters imaged in the experiments shown above. The three tip models are shown in figure 8(b): a sharp tip (I) with a width of about 5 nm at half the height shown, a blunt tip (II) with a width of 17 nm at half height and an asymmetric tip (III) with the same width as the blunt tip, but split into a double tip. In order to calculate the image contrast for such arbitrary shapes, we built the tip and cluster from many thin cylinders and sum the interaction between them [39]. A Hamaker constant of 6.50×10^{-20} J was used, representing the interaction of a silica tip with an insulating surface.

In figure 9 the simulated images of the three different tip–cluster systems are shown for both scanning modes. Images

(a) and (b) show that the sharp tip gives a fairly representative image of the cluster in both imaging modes. The constant height image (b) provides a finer image of the cluster, but the difference is not very significant. Tip convolution is much more clearly demonstrated in the images with the blunt tip, shown in (c) and (d). Although the outline of the cluster can be estimated at the centre of the image, convolution of the blunt tip with the cluster causes the contrast to be smeared out. Here the difference between the imaging modes is more pronounced, with the constant height image being closer to the real lateral cluster size, if not the lateral shape.

For the asymmetric tip, the topography image (e) clearly shows the effect of the double apex. The outline of the cluster can be seen, with a similar, but extended, contrast to that of the sharp tip shown in (a) at the centre of the image. However, the lower part of the image shows that the cluster is effectively imaged again by the second apex, producing a weak shadow contrast feature. However, the detuning image gives a much better representation of the lateral cluster shape (f).

The simulations clearly demonstrate that in the constant height mode the convolution effect of the tip can be significantly reduced for blunt and asymmetric/multiple tips. Sharp tips, however, provide an excellent image of the cluster in either mode. In terms of multiple tips, the simulations agree well with experiments—the measurements shown in figure 5 exactly represent qualitatively what is demonstrated in simulations shown in figures 9(e) and (f).

However, for the images shown in figures 3 and 4 it is also clear that none of these simplistic tip models reproduce the difference between the two modes. The simulations lead us to another, more complex model, which probably explains the high contrast of clusters in our images and which was already introduced in atomic resolution imaging [23]. It is clear that the tip apex is not smoothly round as in the case of our tip models, but rather composed by one or several microscopic small *nanotips*. Since only the sharp tip (I) yields a strong contrast in the simulations (figures 9(a) and (b)), we strongly anticipate that mainly nanotips, which might have even smaller size than the sharp tip (I), contribute to the contrast formation of clusters in the constant height mode.

Analysis of detuning versus distance curves over the NaCl surface (1) and a cluster (2), which is shown in figure 10(a), demonstrates that the tip–surface interaction experiences a rapid increase as the tip approaches close to contact—characteristic of short range chemical and van der Waals forces. Since the high resolution constant height images of the clusters were generated in this strong interaction region (substrate $\Delta f_{\mathrm{Substrate}} = -51$ Hz, cluster $\Delta f_{\mathrm{Cluster}} = -95$ Hz $\approx 2 \times \Delta f_{\mathrm{Substrate}}$), this suggests that contrast is dominated by the short range interaction of a nanotip (or nanotips) with the cluster. During scanning in the constant height mode, the tip is moved at constant height above the clusters so that the strong tip–cluster interaction drastically drops from $\Delta f_{\mathrm{Cluster}}$ to $\Delta f_{\mathrm{Substrate}}$ as soon as the tip passes the cluster due to the much larger tip–substrate surface distance (figure 10(b)).

The model we propose here shows qualitatively that the lateral cluster size and shape is likely determined by the nanotip since it is only the nanotip which is located in the short range tip–cluster interaction and not the blunt part of the tip. This is also supported by our preliminary results

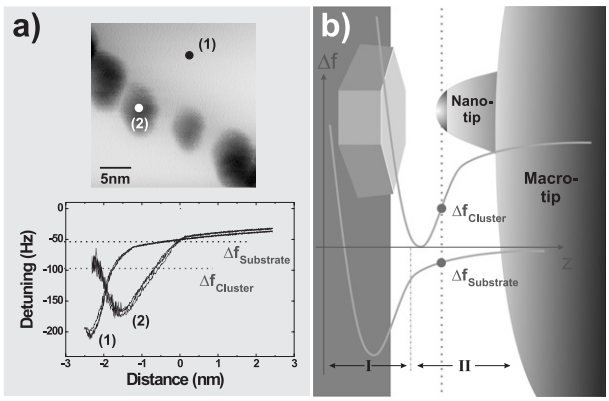

Figure 10. (a) The same image as shown in figure 6(b). Below: detuning versus distance curves taken above the NaCl(001) surface (1) and the cluster (2) (zero point of z-axis arbitrarily chosen). Three $\Delta f(z)$ curves were taken for each surface site. (b) Drawing explaining the contrast formation of clusters in the constant height mode. The tip keeps a pathway with constant height as shown by the thick dotted line. The upper $\Delta f(z)$ curve is the one when the tip is above the cluster, the lower curve for the case in which the tip is above the substrate surface. The region I in the lower $\Delta f(z)$ curve is the one of the short range tip–surface interaction; region II marks the long range, macroscopic tip–surface interaction.

from simulations including the chemical interaction. The tip convolution effect would therefore be reduced to an amount comparable to the size of the nanotip which can have sizes of only a few nanometres or, in the best case, some ångströms. Further, it means that high resolution can also be achieved with blunt tips as soon as they carry a nanotip. However, if the tip is scanned in the constant Δf or I mode, the macroscopic parts of the tip also interact, reducing the accuracy in the images.

5. Summary and discussion

For the first time, we show high quality images of metal nanoclusters which were recorded in the constant height mode of the dynamic SFM. The Au/HOPG system was taken since it provides metal clusters with well defined and symmetric shapes suitable for a characterization of the constant height mode.

Images recorded in the constant height mode show a much better quality in comparison to images recorded in the constant Δf mode, with the clusters exhibiting more reasonable lateral cluster shapes and sizes in comparison to TEM images. Due to the high scanning speeds, the constant height mode minimizes the influence of instrumental drift in the images. We demonstrate that the constant height mode can also be used for surfaces of a non-conducting material such as Au/NaCl(001).

In order to understand the imaging process and to verify to what extent the tip convolution effect can be reduced, we performed numerical simulations with a sharp, blunt and double tip based on a van der Waals tip–cluster interaction. The simulations show that for blunt tips which exceed cluster sizes an improvement of the image resolution can be seen. Only sharp tips with sizes equal to the cluster sizes or even smaller tips yield a high resolution. We believe that especially small microscopic parts of the tip apex, so called *nanotips*, mainly contribute to the image contrast.

To our mind, the results presented here form a large step forward in the microscopy of metal nanoclusters which is very important for the characterization of the cluster structure and morphology in catalysis. In future we will perform further comparisons between calculated and experimental images of similar clusters with an additional comparison with TEM in order to unambiguously prove our model of nanotips. The most ambitious objective is, however, to receive high resolution on top of the clusters, e.g. atomic resolution in this specific mode.

Acknowledgments

We thank L Tocco for stimulating discussions. This work was supported by the European Community through the STRP GSOMEN. Olli H Pakarinen and Adam S Foster are grateful to the Academy of Finland and the TEKES project SURFOX for funding.

References

[1] Henry C R 2003 Reaction dynamics on supported metal clusters *Surface Dynamics* ed D P Woodruff (Amsterdam: Elsevier Science) p 247
[2] Henry C R 2003 Adsorption and reaction at supported model catalysts *Catalysis and Electrocatalysis at Nanoparticle Surfaces* ed A Wieckowski, E R Savinova and C G Vayenas (New York: Dekker) p 239
[3] Henry C R 1998 *Surf. Sci. Rep.* **31** 231
[4] Valden M, Lai X and Goodman D W 1998 *Science* **281** 1647
[5] Morita S, Wiesendanger R and Meyer E 2002 *Noncontact Atomic Force Microscopy* (Berlin: Springer)
[6] Giessibl F J 2003 *Rev. Mod. Phys.* **75** 949
[7] Hofer W A, Foster A S and Shluger A L 2003 *Rev. Mod. Phys.* **75** 1287
[8] Fererro S, Piednoir A and Henry C R 2001 *Nano Lett.* **1** 227
[9] Højrup-Hansen K, Ferrero S and Henry C R 2004 *Appl. Surf. Sci.* **226** 167
[10] Xu S and Arnsdorf M F 1994 *J. Microsc.* **173** 199
[11] Wilder K, Quate C, Singh B, Alvis R and Arnold W H 1996 *J. Vac. Sci. Technol.* B **14** 4004
[12] Castle J E and Zhdan P A 1997 *J. Phys. D: Appl. Phys.* **30** 722
[13] Ferrero S, Højrup-Hansen K and Henry C R 2005 *Surf. Sci.* submitted
[14] Villarrubia J S 1997 *J. Res. Natl Inst. Stand. Technol.* **102** 425
[15] Todd B A and Eppell S J 2001 *Surf. Sci.* **491** 473
[16] Pang C L, Raza H, Haycock S A and Thornton G 2000 *Surf. Sci.* **460** L510
[17] Haas G, Menck A, Brune H, Barth J V, Venables J A and Kern K 2000 *Phys. Rev.* B **61** 11105
[18] Tait S L, Ngo L T, Yu Q M, Fain S C and Campbell C T 2005 *J. Chem. Phys.* **122** 64712
[19] Barth C and Henry C R 2004 *Nanotechnology* **15** 1264
[20] Pakarinen O H, Barth C, Foster A S, Nieminen R M and Henry C R 2005 *Phys. Rev.* B submitted
[21] Bryant A, Smith D P E and Quate C F 1986 *Appl. Phys. Lett.* **48** 832
[22] Wiesendanger R 1998 *Scanning Probe Microscopy and Spectroscopy* (Cambridge: Cambridge University Press)
[23] Barth C, Foster A S, Reichling M and Shluger A L 2001 *J. Phys.: Condens. Matter* **13** 2061
[24] Grange G and Mutaftschiev B 1975 *Surf. Sci.* **47** 723
[25] Grange G, Landers R and Mutaftschiev B 1976 *Surf. Sci.* **54** 445
[26] Barth C, Claeys C and Henry C R 2005 *Rev. Sci. Instrum.* **76** 83907
[27] Barth C and Henry C R 2006 *Nanotechnology* **17** S155–61
[28] Meyer G and Amer N M 1988 *Appl. Phys. Lett.* **53** 1045
[29] Howald L, Meyer E, Lüthi R, Haefke H, Overney R, Rudin H and Güntherodt H J 1993 *Appl. Phys. Lett.* **63** 117
[30] Albrecht T R, Grütter P, Horne D and Rugar D 1991 *J. Appl. Phys.* **69** 668
[31] Omicron SCALA *Technical Reference and Software Manuals*
[32] Couturier G, Boisgard R, Dietzel D and Aimé J P 2005 *Nanotechnology* **16** 1346
[33] Lüthi R, Meyer E, Bammerlin M, Baratoff A, Lehmann T, Howald L, Gerber Ch and Güntherodt H J 1996 *Z. Phys.* B **100** 165
[34] Fain S C Jr, Polwarth C A, Tait S L, Campbell C T and French R H 2006 *Nanotechnology* **17** S121–7
[35] Kern R, Le Lay G and Métois J-J 1979 *Current Topics in Material Science 3* vol 3, ed E Kaldis (Amsterdam: North-Holland) chapter 3, p 139
[36] Humbert A, Pierrisnard R, Sangay S, Chapon C, Henry C R and Claeys C 1989 *Europhys. Lett.* **10** 533
[37] Granjeaud S, Yckache K, Dayez M, Humbert A, Chapon C and Henry C R 1993 *Microsc. Microanal. Microstruct.* **4** 409
[38] Chapon C, Granjeaud S, Humbert A and Henry C R 2001 *Eur. Phys. J. A. P.* **13** 23
[39] Cooper K, Gupta A and Beaudoin S 2001 *J. Colloid Interface Sci.* **234** 284